

Chemical Science

Accepted Manuscript

This article can be cited before page numbers have been issued, to do this please use: J. Zhang, T. Liu, X. Dong, Z. Chen, B. Tang, F. Bu, H. Li, Z. Zhou, D. Chao and R. Zhao, *Chem. Sci.*, 2026, DOI: 10.1039/D5SC08605A.



This is an Accepted Manuscript, which has been through the Royal Society of Chemistry peer review process and has been accepted for publication.

Accepted Manuscripts are published online shortly after acceptance, before technical editing, formatting and proof reading. Using this free service, authors can make their results available to the community, in citable form, before we publish the edited article. We will replace this Accepted Manuscript with the edited and formatted Advance Article as soon as it is available.

You can find more information about Accepted Manuscripts in the [Information for Authors](#).

Please note that technical editing may introduce minor changes to the text and/or graphics, which may alter content. The journal's standard [Terms & Conditions](#) and the [Ethical guidelines](#) still apply. In no event shall the Royal Society of Chemistry be held responsible for any errors or omissions in this Accepted Manuscript or any consequences arising from the use of any information it contains.

Electrolyte Coordination Environments in Wide-Temperature Aqueous Metal Batteries: Mechanisms and Design Strategies

Jiashuo Zhang ^{a,b}, Tao Liu ^{a,b}, Xusheng Dong ^{a,b}, Zhongju Chen ^{a,b}, Bin Tang ^a, Fanxing Bu ^c, Hongpeng Li ^d, Zhen Zhou ^a, Dongliang Chao ^{c*}, Ruizheng Zhao ^{a,b,e*}

- ^a Interdisciplinary Research Center for Sustainable Energy Science and Engineering (IRC4SE²), Engineering Research Center of Advanced Functional Material Manufacturing of Ministry of Education, School of Chemical Engineering, Zhengzhou University, Zhengzhou 450001, Henan, China.
 - ^b Salt Lake Chemical Engineering Research Complex, Qinghai University, Qinghai 810016, Gansu, China
 - ^c Laboratory of Advanced Materials, Aqueous Battery Center, Shanghai Wusong Laboratory of Materials Science, College of Smart Materials and Future Energy, Fudan University, Shanghai 200433, Shanghai, China
 - ^d College of Mechanical Engineering, Yangzhou University, Yangzhou 225127, China
 - ^e National Key Laboratory of Special Rare Metal Materials, Zhengzhou University
- *Corresponding author: rzzhao@zzu.edu.cn (R. Zhao); chaod@fudan.edu.cn (D. Chao)



Abstract

View Article Online
DOI: 10.1039/D5SC08605A

Aqueous metal batteries (AMBs) are promising for energy storage attributed to intrinsic safety, low cost, and environmental friendliness. However, they degrade at extreme temperatures, *i.e.*, crystallization at low temperature and evaporation or heat-driven side reactions at high temperature that have raised performance and safety concerns. Solving these challenges requires simultaneous thermodynamic and kinetic insights of electrolyte behavior under such conditions. Among various strategies, tuning intermolecular interactions to optimize the electrolyte coordination environments has been proven to be especially effective. Yet, comprehensive treatments that integrate both low- and high-temperature regulation with underlying the electrochemical mechanisms remain scarce. This review (i) dissects the failure modes of AMBs under extreme temperature conditions, (ii) synthesizes advances in molecular-interaction tuning for wide-temperature performance, and (iii) offers perspectives and design guidelines for future research and development.

Keywords: Aqueous metal batteries, wide-temperature, intermolecular interactions, coordination environments, electrochemical mechanisms.



1. Introduction

As the demands for electrochemical energy storage grow, aqueous metal batteries (AMBs) have gained attention as low-cost, intrinsic safety, and eco-friendliness with high energy density^[1-5]. AMBs already serve portable electronics^[6-10], yet their performance in extreme environments (*e.g.*, polar and aerospace settings) is constrained by electrolyte phase transition^[11-15]. The thermal stability of aqueous electrolytes is determined by the solvation/coordination structure shaped by intermolecular interactions^[16-21]. At low temperatures ($< -20^{\circ}\text{C}$), the elevated desolvation energy would impede ion transport, while strengthened hydrogen bonding (HB) among free water molecules can induce crystallization. At high temperatures ($> 60^{\circ}\text{C}$), weakened solvation structures may cause solute decomposition and parasitic reactions^[22-27]. Thus, regulating intermolecular interactions to optimize the coordination environments is essential for electrolytes that operate reliably at wide-temperature.

Various strategies have been proposed to overcome the dilemma of the wide-temperature adaptability of AMBs, but optimizing the electrolyte remains a core challenge (**Fig. 1a**)^[28-32]. The solvation-structure framework, *i.e.* the connection between intermolecular interactions and the electrolyte coordination environment, is a key approach for understanding and designing AMBs^[33-38]. Some researchers have reviewed the solvation process and emphasized its significant impact on electrochemical performance. These effects are intensified at low temperature due to sluggish ion kinetics, higher viscosity, and crystallization^[39,40]. To mitigate them, polar additives and highly concentrated electrolytes have been employed to modulate intermolecular interactions and reshape coordination environments^[41,42]. For example, MgCl_2 has been used in aqueous magnesium-based batteries, where the Cl^- adjusts the coordination environment, lowering desolvation energy and freezing point^[43]. However, this approach can raise safety concerns at high temperatures: accelerated transport may trigger electrolyte decomposition, evaporation, and Cl^- oxidation, causing pH shifts, corrosion, and parasitic reactions^[44]. Currently high-temperature strategies typically employ flame retardants, thermally stable salts, or solid-state electrolytes to suppress evaporation and enhance safety^[45-47]. Overall, many methods work only within narrow temperature windows and rely heavily on composition tuning, often without mechanistic clarity on how molecular interactions govern thermal



stability^[48-53]. Therefore, designing wide-temperature electrolytes demands systematic regulation of molecular-level interactions and coordination structures to balance low- and high-temperature performance.

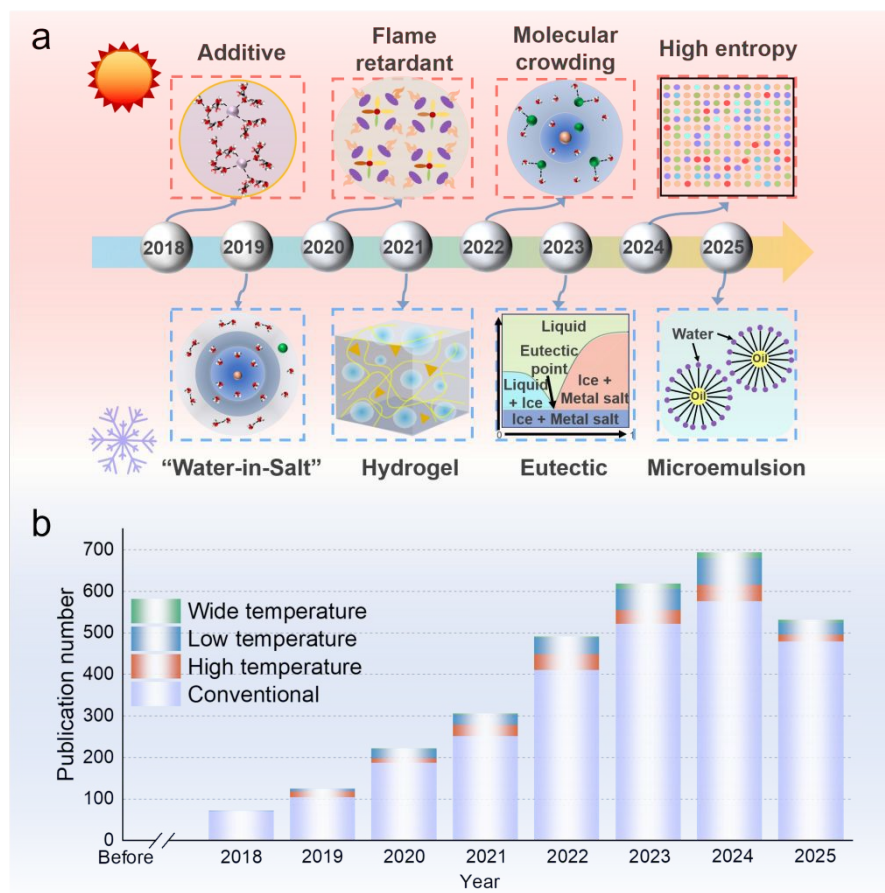


Fig. 1. (a) Timeline of key milestones in engineering in wide-temperature AMBs. (b) Number of publications at wide-temperature AMBs.

Recent atomic-level reviews have advanced our understanding of ion transport in AMBs. These studies have systematically analyzed low-temperature electrolyte regulation through atomic insights, and proposed molecular-design principles for one specific kind of all-weather aqueous metal batteries^[22, 54]. However, the existing reviews typically address either high- or low-temperature regimes—or focus on a specific battery type—without an integrated wide-temperature perspective (**Fig. 1b**). This review fills that gap by centering on regulation of the electrolyte coordination environment *via* tailored molecular interactions. Unlike the traditional perspective, we designed a “moderate solvation structure” by regulating the intermolecular forces. This strategy is not limited to the regulation of a certain type of AMBs, nor is it confined to



high or low temperatures. This regulatory strategy targets the delicate balance of interactions between solvent, cations and anions rather than relying on one-dimensional modifications to intermolecular forces or the selective tuning of specific types of AMBs. Furthermore, this method is not confined to enhancing the battery's performance at high or low temperatures, it can be applied at wide-temperatures. We systematically examine the governing mechanisms, synthesize design strategies for stable performance across a broad temperature range, and offer practical recommendations to guide future wide-temperature AMBs development.

2. Challenges of AMBs at extreme temperatures

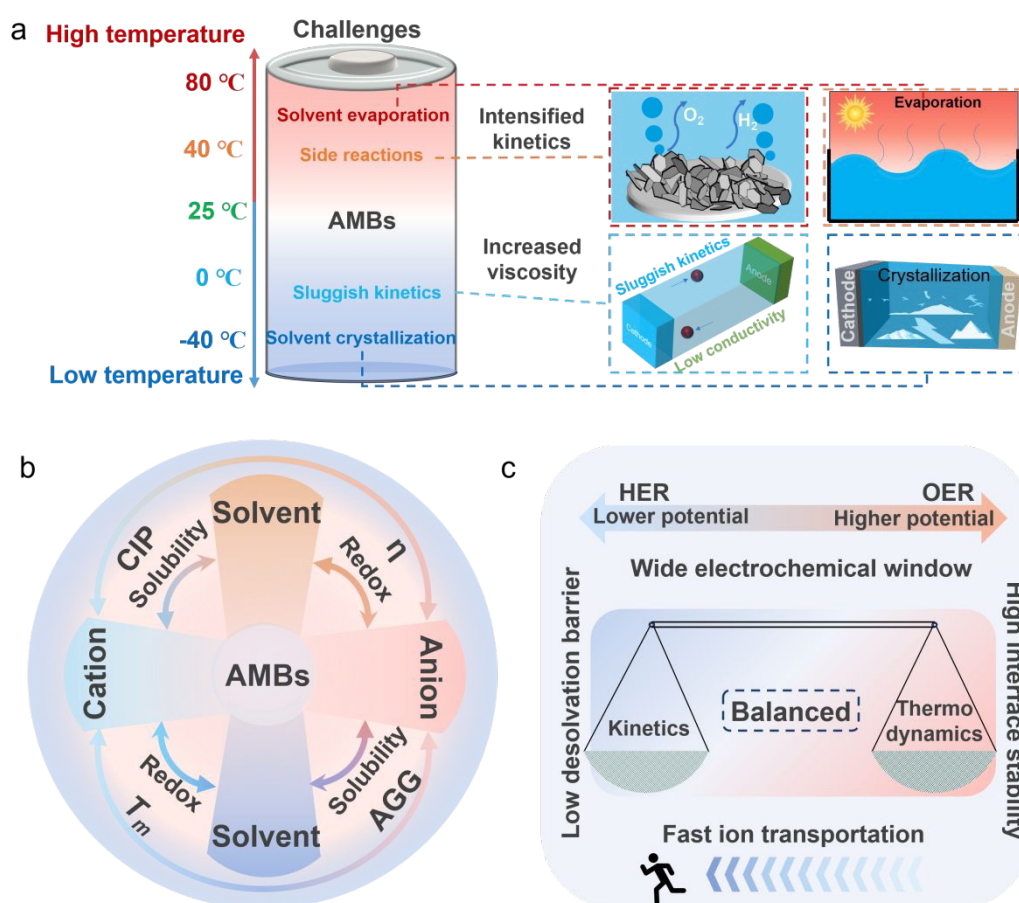


Fig. 2. (a) High- and low- temperature challenges of AMBs. (b) Electrolyte-component interaction map (T_m : melting point; η : viscosity; CIP: Contact ion pair; AGG: Aggregates). (c) Kinetics and thermodynamics equilibrium.

Despite the advantages of AMBs in safety, cost, and environmental sustainability, AMBs still face critical challenges (**Fig. 2a**). Beyond common issues such as dendrite



formation and gas evolution, temperature-induced failures, such as electrolyte crystallization, performance degradation caused by extremely sluggish kinetics at low temperatures, thermal runaway and decomposition caused by poor thermodynamics at high temperatures, remain major barriers achieving wide-temperature operation. Unlike the conventional organic-based batteries, aqueous-based batteries contain a large amount of free water molecules with high reactivity, whose intrinsic physicochemical properties compromise electrolyte stability under extreme conditions. These challenges are closely linked to the molecular interactions that govern the electrolyte's coordination environment (**Fig. 2b**). Therefore, this section provides a comprehensive overview of the key failure modes in AMBs at extreme temperatures elucidating the underlying thermodynamic and kinetic mechanisms, highlighting the significant impact of changes in intermolecular forces drive these behaviors (**Fig. 2c**)^[55].

2.1 Low temperature thermodynamic analysis

From a thermodynamic perspective, the main challenge of low-temperature electrolytes is crystallization. The solid–liquid phase transition is governed by changes in the Gibbs free energy (ΔG), described by following equation:

$$\Delta G = \Delta H - T\Delta S \quad (1)$$

where ΔH , T , and ΔS refer to the enthalpy change, the absolute temperature in K, and the entropy change of the electrolyte actual system, respectively^[56,57]. When $\Delta G = 0$, the electrolyte system undergoes an equilibrium phase transition process^[58]. The temperature at which the electrolyte reaches this point T_m , is the solid–liquid phase transition temperature, and T_m depends on the ratio of the enthalpy change, ΔH to the entropy change, ΔS , as denoted in the equation:

$$T_m = \frac{\Delta H}{\Delta S} = \frac{H_{soln} - H_{ice} - H_{M \cdot nH_2O}}{S_{soln} - S_{ice} - S_{M \cdot nH_2O}} \quad (2)$$

where H_{soln} , H_{ice} , and $H_{M \cdot nH_2O}$ represent the enthalpies of the solution, that of the ice, and hydrated salt $M \cdot nH_2O$, respectively. S_{soln} , S_{ice} , and $S_{M \cdot nH_2O}$ are the entropies of the solution, that of the ice, and $M \cdot nH_2O$, respectively.

As the temperature decreases, the thermal motion of water molecules weakens, stable hydrogen bonds take precedence and liquid water gradually turns into ice. Water transforms from a short-range ordered tetrahedral structure in a liquid state to a long-range ordered hexahedral structure^[59-61]. The constraints of the degrees of freedom of molecular motion and the formation of long-range ordered structures lead to a significant reduction in structural entropy, raising the T_m ^[62,63]. Since the enthalpy and



entropy of ice and solutes are relatively constant, therefore maintaining the electrolyte in a liquid state at low temperature requires a solution with lower ΔH and higher ΔS ^[64,65]. Introducing strongly polar molecules or cosolvents can reduce ΔH by releasing heat through intermolecular interactions and simultaneously disrupt the HB network and coordination environment, increasing system entropy^[66,67]. Therefore, creating a multi-component solvation structure that regulates the HB network and coordination environment is an effective strategy of stabilizing aqueous electrolytes at low temperatures.

2.2 Low temperature kinetic analysis

In addition to thermodynamic limitations, kinetic factors such as desolvation, polarization, and charge transfer also significantly affect the performance of AMBs at low temperatures^[68,69]. During the desolvation process, higher solvation energy leads to greater energy barrier, which hinders the dissolution of metal ions. At low temperatures, the reduced thermal motion and molecular freedom increase intermolecular interactions, promoting the formation of stable coordination structures and further elevating solvation energy and impeding ion dissolution^[70,71]. Additionally, the ionic conductivity (σ) that depends on ion concentration (n_i), mobility (μ_i), unit charge (e), and valence (z), is adversely affected. Moreover, the strong interactions within large solvation clusters restrict molecular mobility, increasing electrolyte viscosity^[72,73]. As a result, the associated ionic conductivity (σ) also decreases as a function of temperature. Among them, ion concentration is determined by salt content, ion mobility is inversely related to viscosity (η) and the radius (r) of solvated metal ions, following the Stokes–Einstein equation:

$$\sigma = \sum_i n_i \mu_i z e \quad (3)$$

$$\mu = \frac{ze}{6\pi\eta r} \quad (4)$$

As temperature decreases, the viscosity of the electrolyte increases, that hinders the ion mobility and reduces electrical conductivity^[74]. The reduction in kinetics caused by these factors will significantly impact battery performance. Take one of the essential performance parameter—voltage for an example, it is also influenced by the solvation structure^[75]. From the perspective of kinetics, operating at low temperatures induces greater battery polarization, including ohmic, concentration, and electrochemical polarization, all of which contribute to a voltage drop. The working voltage (E) of



battery can be described by the following equation:

View Article Online
DOI: 10.1039/D5SC08605A

$$\begin{aligned} E &= E_0 - [(\eta_{ct})_a + (\eta_c)_a] - [(\eta_{ct})_c + (\eta_c)_c] - IR_i E \\ &= E_0 - [(\eta_{ct})_a + (\eta_c)_a] - [(\eta_{ct})_c + (\eta_c)_c] - IR_i \end{aligned} \quad (5)$$

where E_0 represents the voltage, $(\eta_{ct})_a$ and $(\eta_{ct})_c$ represent the activation polarization or ohmic polarization overpotential at the anode or cathode, $(\eta_c)_a$ and $(\eta_c)_c$ represent the concentration polarization overpotential at the anode and cathode respectively. I represents the applied current, and R_i represents the internal resistance. This equation explains that battery voltage is influenced by polarization and internal resistance, both of which are further affected by the coordination environment structure.

At low temperatures, battery polarization can be categorized into three types: (i) Ohmic polarization arises from increased resistance to ion transport. Lower temperatures lead to higher electrolyte viscosity and reduced conductivity, primarily due to the sluggish movement of large solvated clusters. (ii) Concentration polarization occurs when the ion transport rate lags behind the electrode reaction rate, causing ion accumulation or depletion near the electrode surface. This is exacerbated by the slow diffusion of large solvation clusters and high-energy coordination environment structures that hinder ion dissociation and interfacial reactions—especially under high current densities. (iii) Electrochemical polarization results from sluggish interfacial charge transfer. At low temperatures, the increased activation energy for ion desolvation and electrochemical reactions slows down the electron transfer kinetics, requiring higher overpotentials to sustain the reaction^[76,77]. In summary, achieving stable aqueous electrolyte at low temperatures requires balancing thermodynamic and kinetic factors. This can be realized by regulating intermolecular interactions to construct a robust coordination environment structure with favorable physicochemical properties.

2.3 High temperature thermodynamic analysis

Unlike at low temperatures, where the main thermodynamic challenge is insufficient energy (*e.g.*, high dissolution barriers and electrolyte crystallization), high-temperature conditions present the opposite problem, *viz.* excess energy. This leads to thermal decomposition and electrolyte evaporation^[78,79]. One of the earliest consequences of elevated temperatures is the narrowing of the electrolyte's electrochemical stability window (ESW), which is defined by its oxidation potential (E_{ox}) and reduction potential (E_{red}). High temperatures alter the equilibrium potential of electrode surface reactions,



thereby directly reducing the ESW^[80-82]. For example, in the case of oxygen evolution, View Article Online
DOI: 10.1039/D5SC08605A



The equilibrium potential E_{ox} can be described by the Nernst equation:

$$E_{ox} = E_{ox}^0 - \frac{RT}{nF} \ln \left(\frac{a_{H_2O}}{a_{O_2} a_{H^+}^4} \right) \quad (7)$$

Here, E_{ox}^0 is the standard equilibrium potential, and a_{H_2O} , a_{O_2} , a_{H^+} are the activities of H_2O , O_2 and H^+ , respectively. As the temperature increases, the thermal motion of water molecules intensifies, weakening the HB network and increasing the activity of free water molecules. Meanwhile, gas solubility decreases at higher temperatures (according to Henry's law: Under certain temperature and equilibrium conditions, the solubility of a gas in a liquid is directly proportional to the equilibrium partial pressure of the gas.), reducing the activity of dissolved oxygen due to its escape from the electrolyte. Consequently, the term $\frac{RT}{nF} \ln \left(\frac{a_{H_2O}}{a_{O_2} a_{H^+}^4} \right)$ increases, shifting E_{ox} to lower potentials, thereby narrowing the electrochemical stability window and making oxygen evolution reactions more prone^[83,84]. Thermodynamically, elevated temperatures enhance the thermal energy of electrons, increasing the likelihood of transitions to higher energy levels^[85,86]. Additionally, this also affects the electrolyte's solvation structure: weaken the dipole-dipole interactions between solvent molecules and reducing solvation stability^[87,88]. Moreover, the increased thermal agitation raises the probability of electron transitions from the HOMO to the LUMO or higher excited states, effectively narrowing the energy gap. This promotes side reactions at the electrodes interface, leading to the growth of a thicker solid electrolyte interphase (SEI). The thickened SEI further depletes electrolyte components and hinders efficient ion transport across the electrode-electrolyte interface^[89,90].

2.4 High temperature kinetic analysis

At low temperatures, the primary challenges are high dissolution energy barriers and sluggish ion transport. In contrast, these limitations are largely alleviated at high temperatures^[91-93]. According to the Stokes-Einstein equation, self-diffusivity is inversely related to viscosity:

$$D = \frac{kT}{6\pi\eta r} \quad (8)$$

where D is the self-diffusion coefficient. As the temperature T increases, η decreases



and D increases, highlighting their inverse relationship. This promotes ion mobility and benefits the kinetics behavior of the electrolyte^[94,95]. However, while elevated temperatures enhance ion transport, they also significantly accelerate the side reactions. Unlike the narrowing of the ESW mentioned above, the increase in temperature accelerates the rates of hydrogen and oxygen evolution reactions and the decomposition of the electrolyte, disrupting the thermodynamic and kinetic balance. Moreover, the products of these side reactions will cause a large accumulation of gas and an imbalance in the pH of the electrolyte, leading to the decomposition of the SEI and severe electrode corrosion. This will cause further deterioration of the electrolyte, resulting in rapid battery failure. According to the Arrhenius equation, the reaction rate constant (k) is given by:

$$k = A \exp\left(-\frac{E_a}{RT}\right) \quad (9)$$

Where E_a is the activation energy, and A is the pre-exponential factor. As the temperature increases, the term $\exp\left(-\frac{E_a}{RT}\right)$ increase, significantly accelerating side reaction rates^[96,97]. Most of the side reactions are exothermic, and if the heat generated is not effectively dissipated, it can lead to rapid battery degradation and even trigger thermal runaway, posing serious safety risks^[98,99]. In summary, while elevated temperatures can enhance battery performance by improving ion transport and reaction kinetics, they also intensify thermodynamic instability. Achieving stable and safe operation under high-temperature conditions requires careful balancing of thermodynamic and kinetic factors. Therefore, the design of thermally robust coordination environment structures is essential for high-temperature aqueous electrolytes.

3. Mechanism and design strategies for wide-temperature AMBs

Tailoring the electrolyte coordination environment is a promising strategy to mitigate the performance limits of AMBs at extreme temperatures. That environment is governed by three interdependent interactions, *i.e.*, solvent–solvent, solvent–ion, and ion–ion, that together set the electrolyte’s physicochemical properties. Effective regulation therefore requires precise, targeted modulation of these interactions. In this section, we examine atomic-scale mechanisms for designing wide-temperature aqueous electrolytes *via* controlled tuning of intermolecular interactions.



3.1 Regulation of solvent–solvent interactions

Regulating solvent–solvent interactions in AMBs mainly means modulating water–water HB. Each H_2O can form up to four HBs (two donor H atoms and two acceptor lone pairs), producing an extended tetrahedral network (**Fig. 3a**). At low temperatures this ordered network promotes crystallization and electrolyte freezing; at high temperatures increased molecular motion disrupts HB and accelerates evaporation. Therefore, disrupting or reconfiguring the intrinsic HB network is essential to stabilize aqueous electrolytes across a wide temperature range.

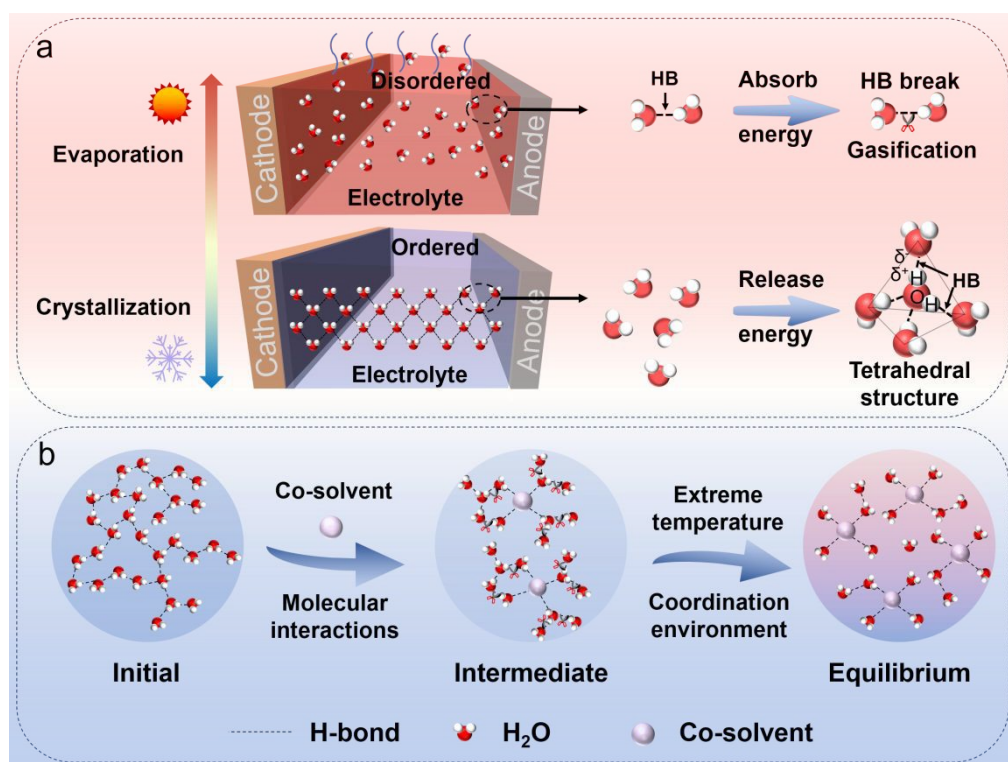


Fig. 3. (a) Water-related failure modes in AMB electrolytes at low and high temperatures. (b) Schematic of temperature-driven changes in the electrolyte coordination environment.

A common approach is to introduce co-solvents or additives, which weakens the HB between water–water, while strengthens the water–co-solvent interactions (**Fig. 3b**)^[100,101]. For instance, Naveed *et al.* used the flame-retardant triethyl phosphate as additive, which stabilizes aqueous zinc batteries (AZBs) at elevated temperatures. However, this additive does not effectively disrupt the HB network, so it only partially suppresses high-temperature decomposition/combustion and offers limited low-temperature protection^[102]. Conversely, Hu's team introduced a quaternized



galactomannan polysaccharide rich in hydroxyl groups, which effectively binds free water and breaks the HB network, enabling operation down to $-30\text{ }^{\circ}\text{C}$, yet its polymeric nature makes it prone to thermal degradation and therefore unsuitable for high-temperature stability^[103].

To disrupt the HB network effectively, co-solvents should form strong hydrogen bonding donor/acceptor (HBD/HBA) interactions with water, preferably stronger than water–water interactions, and multifunctional HB groups further enhance this effect. Typical, water-miscible candidates include sulfoxides, sulfones, nitriles, alcohols, amides, phosphate esters and ketones^[104–110]. An ideal co-solvent therefore should combine the following characteristics: (i) good miscibility with water, (ii) abundant HBA/HBD sites, (iii) high dielectric constant, (iv) chemical and thermal robustness, and (v) low cost. Practical demonstrations support this strategy. A water–eutectic system with ethylene glycol (EG) and SnI_4 enabled a Zn/Zn symmetric cell to run over 6000 h at $-30\text{ }^{\circ}\text{C}$ and 2500 h at $60\text{ }^{\circ}\text{C}$, with MD simulations confirming strong HB disruption by EG^[111]. Similarly, EG-based electrolytes enabled >20 000 cycles at $-40\text{ }^{\circ}\text{C}$ and 10 000 cycles at $105\text{ }^{\circ}\text{C}$ in aqueous Na-ion cells^[112]. These examples show that reconstructing the HB network *via* appropriately chosen co-solvents is an effective route to wide-temperature aqueous electrolytes, suppressing low-temperature crystallization and high-temperature evaporation.

3.2 Regulation of solvent-ion interactions

In addition to regulating the solvent–solvent interaction, the primary aspect is to regulate the solvent–ion interaction. Solvent molecules form metal-ion solvation shells *via* electrostatic solvent–ion interactions, establishing the electrolyte’s coordination structure (**Fig. 4a**). The strength and character of these interactions determine solvation-shell composition and stability, directly govern ion transport and interfacial desolvation (**Fig. 4b**). If solvent–ion coupling is too weak, solvation shells are labile and the HB network persists, degrading low-temperature crystallization resistance and high-temperature stability. Sufficiently strong interactions stabilize the solvation structure and suppress crystallization, but overly strong binding raises desolvation barriers and slows electrochemical kinetics. Therefore, precise tuning of solvent–ion interactions is required to balance thermal robustness and interfacial kinetics. One direct strategy is adjusting electrolyte concentration^[113]. Increasing ion concentration enhances solvent coordination, disrupts HB networks, and stabilizes the solvation shell. For instance, a



highly concentrated $\text{Al}(\text{OTf})_3$ electrolyte was employed by Wang *et al.* in aqueous aluminum batteries (AABs), forming a stable "water-in-salt" coordination structure that effectively disrupted HBs^[114]. However, very high concentrations can increase viscosity and cost, and may lead to crystallization at low temperatures or decomposition at high temperatures. Thus, concentration must be carefully optimized or combined with co-solvents/additives. To address this, Zhang *et al.* formulated a balanced electrolyte using $\text{Al}(\text{OTf})_3$, acetonitrile, triethyl phosphate, and water. The resulting AABs achieved stable operation for 450 h at -10°C and 1500 h at 50°C , demonstrating excellent wide-temperature performance^[89].

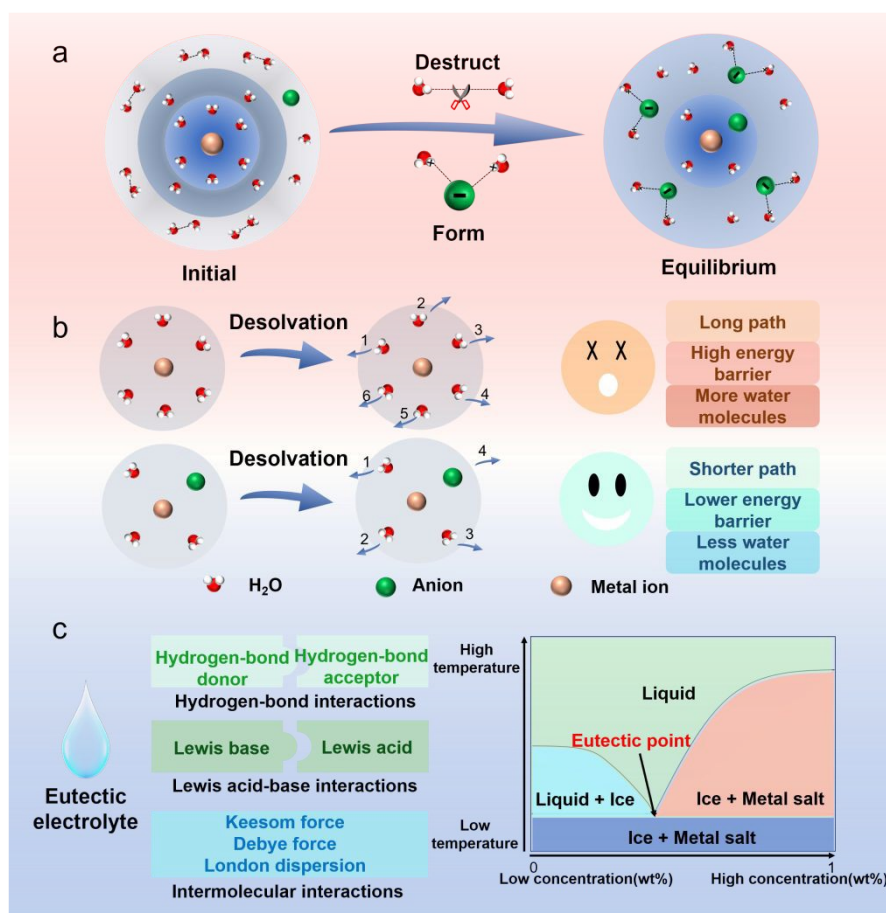


Fig. 4. (a) Ion coordination in electrolytes. (b) Desolvation under different conditions. (c) Principle of eutectic electrolytes.

Another classical approach to strengthen solvent–ion interactions is the use of eutectic electrolytes, which are mixtures of two or more components in specific ratios that exhibit melting points much lower than their individual constituents. Their formation is driven by HB, Lewis acid–base interactions, and van der Waals forces (**Fig.**



4c)^[115]. At the molecular level, eutectic electrolytes emerge from the reconstruction of intermolecular interactions among components, which in aqueous systems disrupts HB network of the water, lower the freezing point, and reduce free-water activity. These effects suppress decomposition reactions at both low and high temperatures and stabilize the solvation environment. For example, Zhang *et al.* developed a hydrated eutectic electrolyte composed of Al(OTf)₃, glycerol, sodium β-glycerophosphate pentahydrate (SG), and water for aqueous aluminum-ion batteries. The Al//Al symmetric cells exhibited excellent cycling stability, operating for over 500 h at −20 °C and 1000 h at 60 °C^[116]. This demonstrates that regulating solvent–ion interactions *via* eutectic systems can “lock” water and construct a stable coordination environment for wide-temperature operation.

3.3 Regulation of cation-anion interaction

Ion transport in electrolytes is primarily governed by solvent–solvent and solvent–ion interactions (**Fig. 5a**). While cation-anion interactions influence the composition and structure of the SEI, which governs interfacial ion transport, therefore cation–anion interactions become critical at the electrolyte–electrode interface^[117,118]. In general, an increase in the content of inorganic components in the SEI film promotes ion diffusion, which is primarily caused by the decomposition of anions in the electrolyte. Strong cation-anion interactions can bring anions closer to the electrode surface, triggering anion decomposition and generating an inorganic-rich SEI layer^[119,120]. The electrolyte’s ion coordination environment determines the priority of which species contribute to SEI formation. A moderate coordination structure favors a dense, homogeneous SEI that suppresses side reactions, enhancing cycling stability and safety. Additionally, a robust SEI mitigates low-temperature embrittlement and cracking as well as high-temperature decomposition or dissolution. However, interfacial ion transport also depends on desolvation: while strong cation–anion interactions improve SEI formation, they may simultaneously increase solvent–ion binding, raising the desolvation energy barrier. In addition, overly strong interactions between cations and anions can lead to the formation of a thick SEI, which not only causes the consumption of electrolyte components but also has an adverse effect on ion transport.



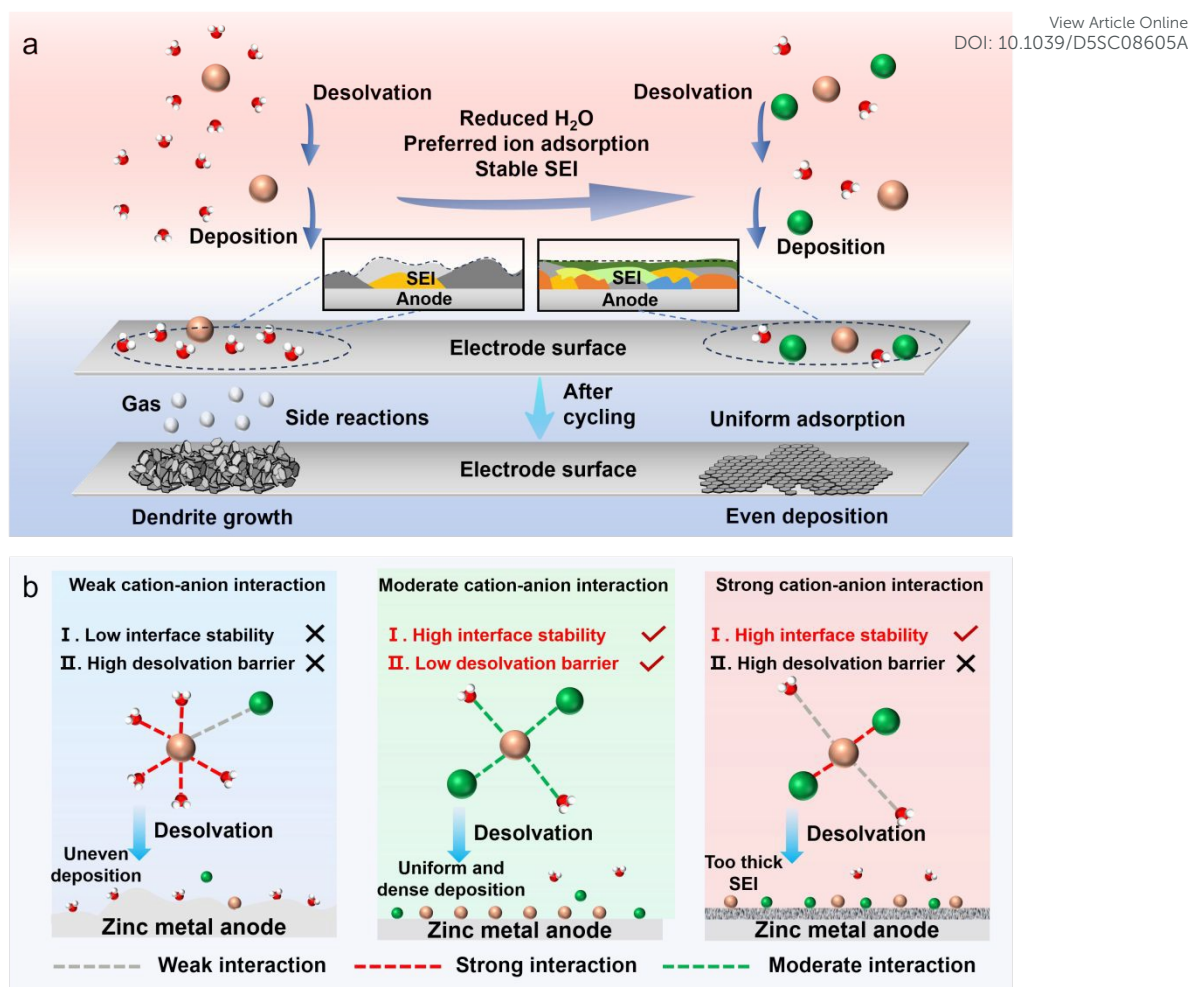


Fig. 5. (a) Deposition of metal ions under different coordination structures. (b) Effects of varying interaction strengths on interfacial processes.

To address this issue, Wang's team introduced bis(2-methoxyethyl)amine (BMEA) as a chelating additive in AABs. The amino group strongly coordinates with metal ions, reshaping the electrolyte's coordination structure and promoting tough cation–anion interactions^[121]. Characterization results confirmed that BMEA participates in SEI formation, contributing to stable battery operation at room temperature. However, at low temperatures, increased desolvation barriers can reduce conductivity, while at high temperatures, excessive SEI growth may deplete the electrolyte. To overcome these limitations, coordination environments should combine strong ion–ion but weak solvent–ion interactions (**Fig. 5b**). The weakly solvated electrolytes was showed by Shi *et al.* that with fewer water molecules in the solvation shell, lower desolvation energy and enable faster ion transport and uniform metal deposition^[122]. Therefore, designing such tailored coordination environments is critical for achieving wide-temperature



electrolyte.

View Article Online
DOI: 10.1039/D5SC08605A

Generally speaking, designing a weak solvation structure requires careful consideration of following several key factors: (i) Solvent polarity, selecting solvents with low dielectric constants to reduce their solvation strength toward metal ions. (ii) Donor ability, choosing solvents with low donor numbers (DN), ideally lower than that of water, to weaken metal ions–solvent coordination. Carbonates and nitriles are common weak interaction solvents that promote the formation of contact ion pairs, facilitating ion desolvation and uniform metal deposition. (iii) Hydrogen bonding, choosing solvents with weak HB donor/acceptor abilities to disrupt the water HB network. (iv) Aprotic solvents, favoring aprotic solvents such as nitriles (*e.g.*, acetonitrile), esters (*e.g.*, methyl acetate), and ethers (*e.g.*, tetrahydrofuran), that act as HB acceptors and help weaken water–water interactions. Xie *et al.* employed γ -valerolactone as a weak solvent, simultaneously enabling AZBs to cycle stably for over 120 cycles at 50 °C and 800 cycles at –30 °C [101]. This solvent acts as a strong HB acceptor and diluent, breaking HB between free water molecules and enhancing both thermal and chemical stability.

In fact, designing wide-temperature electrolytes cannot rely on a single interaction type. Solvent–solvent, solvent–ion, and ion–ion interactions are interdependent, modifying one inevitably affects the others. Therefore, a holistic approach is essential to establish a stable, optimized coordination environment across a broad temperature range.

3.4 Regulation of multiple interactions

Current strategies for regulating the coordination environment in AMBs almost focus on tuning individual intermolecular interactions. Traditional single-solvent systems, limited by uniform interactions that struggle to modulate ion coordination effectively. In contrast, introducing multiple solvent species enables to adjust multiple molecular interactions, producing diverse solvation structures and enhanced electrolyte functionality. This multi-component system used by Zhao *et al.* that contains multiple solvents and/or salts that create a disordered coordination environment that improves battery performance by increasing configurational entropy and weakening electrostatic interactions^[123]. This multi-component approach is captured by the concept of high-entropy electrolytes (HEEs, **Fig. 6a**). Unlike simple solvent mixtures, HEEs require deliberate design to achieve weak solvation, high ionic mobility, and broad



electrochemical stability. Key design principles include (i) good miscibility among solvents for homogeneous solvation, (ii) complementary physicochemical properties to offset individual limitations, and (iii) sufficient salt solubility to support efficient ion transport. For instance, Ji *et al.* utilized a 9 M acetamide-based hybrid solvent in aqueous Zn-metal batteries, achieving over 1000 cycles at $-25\text{ }^{\circ}\text{C}$ and 150 cycles at $50\text{ }^{\circ}\text{C}$ ^[124]. Despite challenges such as structural complexity and higher cost, HEEs demonstrate strong potential for finely tuning coordination environments to achieve high-performance AMBs.

In addition to multi-component systems, maximizing water incorporation into the coordination structure is an effective strategy for wide-temperature electrolytes. Macromolecular polymers, with abundant and regular functional groups, form extensive coordination structures with water. However, their poor solubility limits them to liquid electrolyte applications. To solve this problem, Chen's team utilize hydrogel electrolytes to achieve the advantages of polymers^[125]. Hydrogel electrolytes overcome this problem by combining polymer structural advantages with conductivity of water. Composed of three-dimensional polymer networks, hydrogels retain large amounts of water (**Fig. 6b**), where functional groups, *e.g.*, hydroxyl, carboxyl, amino, form strong HB with water, stabilizing the solvation structure and enabling adaptive coordination across temperatures. These hydrogels are temperature-responsive: at high temperatures, polymer chains coil to reduce free volume and water loss while maintaining ion mobility. At low temperatures, chains re-extend, preserving mechanical flexibility and continuous ion transport. Enhanced HB at low temperatures improves toughness and suppresses embrittlement, ensuring stable electrochemical performance. Optimization can be achieved by introducing functional groups to tune intermolecular interactions (*e.g.*, HB, van der Waals forces) and adjusting crosslink density to strengthen the polymer network. For example, Liu *et al.* developed a double-network polyanionic hydrogel based on borax and bacterial cellulose for Zn//I₂ batteries, achieving over 2000 h of stable cycling at $-50\text{ }^{\circ}\text{C}$ and 600 h at $50\text{ }^{\circ}\text{C}$ under 1 mA cm^{-2} ^[126]. Despite excellent thermal adaptability, hydrogel electrolytes still face challenges in mechanical stability under extreme conditions, requiring further material and structural optimization to enhance durability.



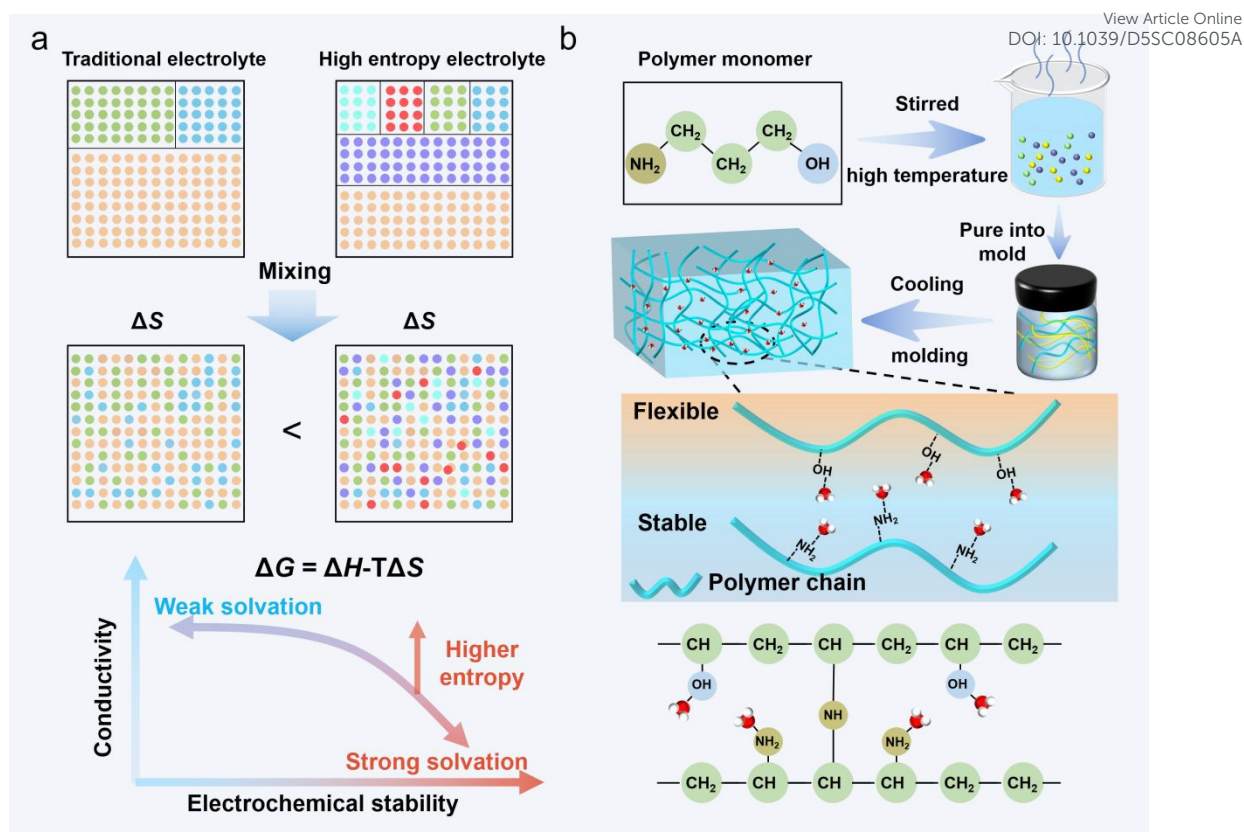


Fig. 6. (a) Schematic of a high-entropy electrolyte. (b) Schematic of a hydrogel electrolyte.

4. Conclusions and perspectives

AMBs are attractive for being low-cost, high security, and environmentally benign, but their aqueous electrolytes suffer from low low-temperature kinetics and unstable high-temperature thermodynamics that restrict wide-temperature operation. This review surveys molecular strategies, tuning solvent-solvent, solvent-ion, and anion-cation interactions that achieve fast low-temperature kinetics and adjust thermodynamics to expand the usable temperature window. Although these approaches have made significant progress, a universally robust wide-temperature aqueous electrolyte has not yet been realized, leaving ample room for further innovation. We therefore outline several priority research directions to advance wide-temperature AMBs (Fig. 7).



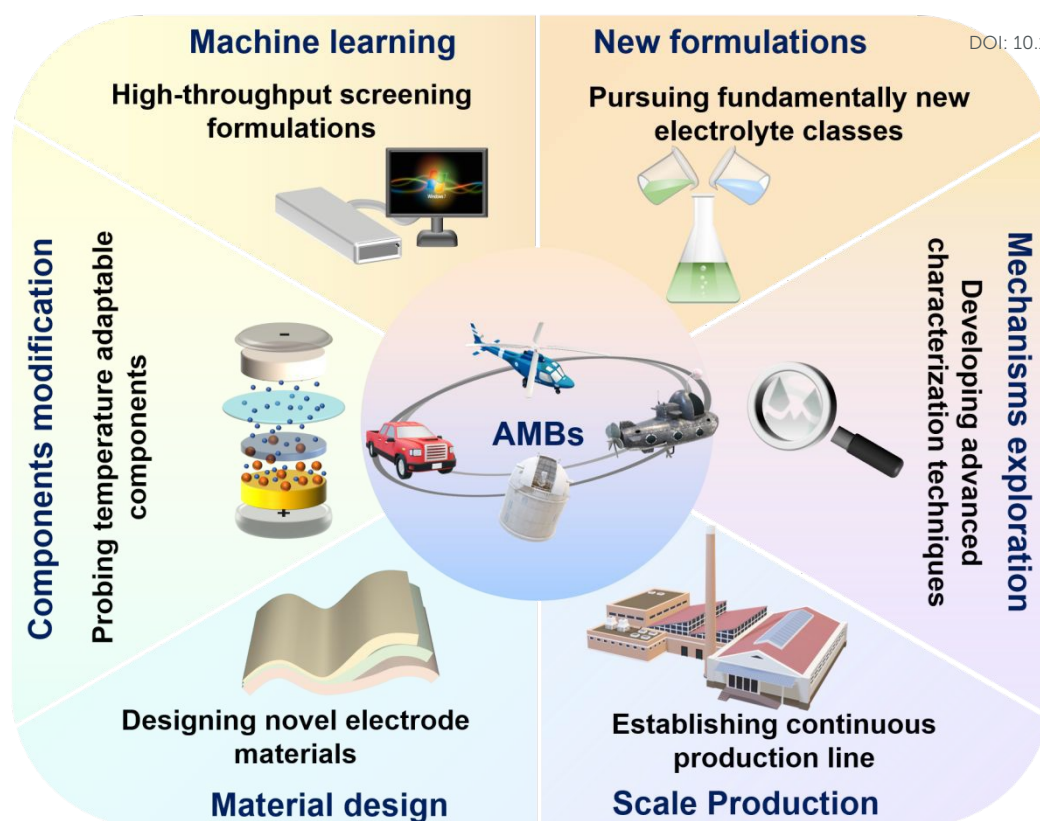


Fig. 7. Future research for the wide-temperature AMBs.

1) Utilize machine learning to screen wide-temperature electrolytes. Compared to traditional methods, machine learning offers faster and more efficient screening of electrolyte materials with varied physical and chemical properties like dielectric constant and viscosity. It can quickly gather extensive data, facilitating the identification of promising electrolytes. Additionally, machine learning can predict key properties such as freezing point, conductivity, and viscosity of prepared electrolytes, guiding more efficient experimental testing.

2) Explore novel electrolytes formulations for wide-temperature AMBs. In order to overcome the inherent instability of conventional aqueous solution systems at extreme temperatures, it is necessary not merely to adjust the proportions of the components, but also pursuing fundamentally new electrolyte classes. Although adjusting component ratios has yielded improvements, traditional aqueous electrolytes still fail under extreme temperatures. Emerging approaches, such as high-entropy and quasi-solid-state aqueous electrolytes, have already shown promise for broader thermal tolerance. However, their stabilizing mechanisms remain lack of understanding. Designing novel electrolyte systems and clarifying the underlying physicochemical



principles will be essential to realize truly wide-temperature aqueous electrolytes.

View Article Online

DOI: 10.1039/D5SC08605A

3) Comprehensively probe mechanisms for wide-temperature AMBs. Although this review systematically examines how various intermolecular forces affect electrolyte properties, most studies consider only one or two interactions in isolation. Coordinated control of multiple intermolecular forces remains underexplored; clarifying their coupled effects requires systematic, multi-variable experiments and multi-scale characterization to extract quantitative parameters. A rigorous, mechanism-first analysis of electrolyte structure and interaction networks is therefore essential for the rational design of aqueous electrolytes that remain stable across wide temperature ranges and for advancing wide-temperature AMBs.

4) Design of novel electrode material for wide-temperature AMBs. At extreme temperatures, common electrode materials suffer accelerated dissolution and capacity loss, while uneven surface electric fields create local high current densities that favor dendrite nucleation. The development of electrodes with wide-temperature adaptability therefore requires high chemical stability such as a stable main structure or protective interface, as well as special structures for uniform charge distribution, such as conformal conductive coatings, engineered porosity, or 3D collectors. Combining these strategies reduces parasitic reactions and dendrite formation, significantly enhancing the cycle life, safety and performance of AMBs at wide-temperature.

5) Optimize separators, binders, and current collectors for wide-temperature AMBs. Secondary components, such as separators, binders and current collectors, have a significant impact on AMB performance, yet they are not widely studied for extreme temperatures. Separators must retain porosity, wettability, and ionic conductivity without mechanical collapse or blockage; binders require thermal and chemical stability while preserving electrode cohesion; and collectors need corrosion resistance and architectures that homogenize current to avoid hotspots and local failure. Systematic development of temperature-adaptive polymers, functional coatings, and structured collectors, together with component-level testing under wide-temperature cycling, is therefore crucial to improving lifetime, safety, and performance of AMBs.

6) Scaling up the production of wide-temperature AMBs. To meet the growing demand for energy storage, it is urgent to scale up the production for wide-temperature AMBs. Although significant progress has been reported in research for wide-temperature AMBs, the technical processes for their large-scale, continuous production



are currently insufficiently developed. In order to strengthen the market position of wide-temperature AMBs, measures must be taken to reduce production costs, optimize production processes and actively develop and promote advanced research technologies. The awareness should also be raised in both the academic and industrial of the wide-temperature AMBs' development to accelerate the large-scale development and production of wide-temperature AMBs as soon as possible and promoting the transformation and development of more efficient energy systems.

Data availability

All data needed to evaluate the conclusions in the paper are present in the Paper.

Conflict of Interest

The authors declare no conflict of interest.

Author contributions

R. Z. and D. C. conceived and supervised the research. J. Z. and T. L. originally drafted and wrote the manuscript. X. D., Z. C. and B. T. provided theoretical guidance. F. B., H. L. and Z. Z. checked and revised the manuscript. All authors discussed the results and commented on the manuscript.

Acknowledgements

This work was financially supported by the National Natural Science Foundation of China (22309165, U24A2060, and 22279023), the National Key R&D Program of China (2024YFE0101100), the Excellent Youth Foundation of Henan Province (242300421126), the Science and Technology Commission of Shanghai Municipality (25DZ3002901 and 25PY2600100), the Talent Development Funding Project of Shanghai (2021030), the Postdoctoral Science Foundation of China (2023M743170), the Key Research Projects of Higher Education Institutions of Henan Province (24A530010), the Open Project of Salt Lake Chemical Engineering Research Complex, Qinghai University (2025-DXSSKF-06), Graduate Student Independent Innovation Project of Zhengzhou University (20250512), and Projects of Innovation and Entrepreneurship Training Programme for College Students of Zhengzhou University (2025cxcy359).



Notes and References

- [1] J. Huang, Z. Guo, Y. Ma, D. Bin, Y. Wang, Y. Xia, *Small Methods*, **2018**, *3*, 1800272.
- [2] L. He, C. Lin, P. Xiong, H. Lin, W. Lai, J. Zhang, F. Xiao, L. Xiao, Q. Qian, Q. Chen, L. Zeng, *Trans. Tianjin Univ.*, **2023**, *29*, 321-346.
- [3] S. Chen, M. Zhang, P. Zou, B. Sun, S. Tao, *Energy Environ. Sci.*, **2022**, *15*, 1805-1839.
- [4] Y. Zhang, L. Zhao, Y. Liang, X. Wang, Y. Yao, *eScience*, **2022**, *2*, 110-115.
- [5] Z. Jiang, X. Yang, J. Zhang, J. Yang, B. Sun, Z. Sun, J. Xue, J. He, Z. Sun, H. K. Liu, S. X. Dou, *Adv. Funct. Mater.*, **2025**, DOI:10.1002/adfm.202511754.
- [6] M. Wang, Y. Meng, Y. Xu, D. Shen, P. Tong, W. Chen, *ACS Energy Lett.*, **2024**, *9*, 1381-1388.
- [7] X. Li, X. Wang, L. Ma, W. Huang, *Adv. Energy Mater.*, **2022**, *12*, 2202068.
- [8] Y. Duan, C. Li, Z. Ye, H. Li, Y. Yang, D. Sui, Y. Lu, *Nanomaterials*, **2022**, *12*, 3954.
- [9] D. Sui, M. Chang, Z. Peng, C. Li, X. He, Y. Yang, Y. Liu, Y. Lu, *Nanomaterials*, **2021**, *11*, 2771.
- [10] D. Sui, M. Wu, Y. Liu, Y. Yang, H. Zhang, Y. Ma, L. Zhang, Y. Chen, *Nanotechnology*, **2021**, *32*, 015403.
- [11] F. Ai, Z. Wang, N.-C. Lai, Q. Zou, Z. Liang, Y.-C. Lu, *Nat. Energy*, **2022**, *7*, 417-426.
- [12] X. Lin, M. Salari, L. M. R. Arava, P. M. Ajayan, M. W. Grinstaff, *Chem. Soc. Rev.*, **2016**, *45*, 5848-5887.
- [13] J. Zhang, C. Lin, L. Zeng, H. Lin, L. He, F. Xiao, L. Luo, P. Xiong, X. Yang, Q. Chen, Q. Qian, *Small*, **2024**, *20*, 2312116.
- [14] L. Jiang, Y.-C. Hu, F. Ai, Z. Liang, Y.-C. Lu, *Energy Environ. Sci.*, **2024**, *17*, 2815-2824.
- [15] Q. Wang, J. He, B. Sun, Y. Bai, Y. Yan, J. Xue, Z. Sun, X. Wang, J. Wu, J. Wang, R. Zhao, Z. Sun, H. K. Liu, S. X. Dou, *ACS Nano*, **2025**, *19*, 28992-29027.
- [16] X. Jin, G. Lai, X. Xiu, L. Song, X. Li, C. Dai, M. Li, Z. Quan, B. Tang, G. Shao, Z. Zhang, F. Liu, L. Qu, Z. Zhou, *Angew. Chem. Int. Ed.*, **2024**, *64*, e202418682.
- [17] J.-W. Zhang, J.-L. Sun, D.-N. Zhao, Y.-J. Zhao, X.-Y. Hu, Y.-N. Wang, Y.-J. Yao, N.-S. Zhang, L.-J. Zhang, C.-L. Li, P. Wang, S.-Y. Li, X.-L. Cui, *Energy Storage Mater.*, **2024**, *72*, 103698.
- [18] B. Sun, F. Huo, C. Zhao, J. He, J. Xue, Z. Sun, J. Wu, X. Wang, J. Wang, R. Zhao, Z. Sun, *J. Mater. Chem. A*, **2025**, *13*, 25444-25456.
- [19] P. Xue, C. Guo, L. Li, H. Li, D. Luo, L. Tan, Z. Chen, *Adv Mater.*, **2022**, *34*, 2110047.
- [20] H. Li, R. Zhao, W. Zhou, L. Wang, W. Li, D. Zhao, D. Chao, *JACS Au*, **2023**, *3*, 2107-2116.
- [21] H. Li, C. Guo, T. Zhang, P. Xue, R. Zhao, W. Zhou, W. Li, A. Elzatahry, D. Zhao, D. Chao, *Nano Lett.*, **2022**, *22*, 4223-4231.
- [22] C. You, W. Fan, X. Xiong, H. Yang, L. Fu, T. Wang, F. Wang, Z. Zhu, J. He, Y. Wu, *Adv. Funct. Mater.*, **2024**, *34*, 2403616.
- [23] X. Zhang, Y. Liu, S. Wang, J. Wang, F. Cheng, Y. Tong, L. Wei, Z. Fang, J. Mao, *Energy Storage Mater.*, **2024**, *70*, 103471.
- [24] Y. Lv, Y. Xiao, L. Ma, C. Zhi, S. Chen, *Adv Mater.*, **2021**, *34*, 2106409.
- [25] X. Gao, J. Yang, Z. Xu, Y. Nuli, J. Wang, *Energy Storage Mater.*, **2023**, *54*, 382-402.
- [26] C. Cao, S. Tang, X. Wu, H. Huang, S. Liu, H. Li, *Adv. Sci.*, **2025**, DOI:10.1002/advs.202511439.
- [27] H. Li, S. Ding, J. Ding, J. Luo, S. Liu, H. Huang, *Energy Storage Mater.*, **2025**, *74*, 103907.
- [28] T. Liu, X. Dong, B. Tang, R. Zhao, J. Xu, H. Li, S. Gao, Y. Fang, D. Chao, Z. Zhou, *J. Energy Chem.*, **2024**, *98*, 311-326.



- [29] M. Wang, Z. Xu, C. He, L. Cai, H. Zheng, Z. Sun, H. K. Liu, H. Ying, S. Dou, *ACS Nano*, **2025**, *19*, 9709-9739. View Article Online
DOI: 10.1039/D5SC08605A
- [30] R. Zhao, A. Elzatahry, D. Chao, D. Zhao, *Matter*, **2022**, *5*, 8-10.
- [31] J. Xu, T. Liu, X. Dong, X. Dong, W. Zhou, X. Li, D. Chao, Z. Zhou, R. Zhao, *Natl. Sci. Rev.*, **2025**, *12*, nwae433.
- [32] Z. Xie, Y. Qu, F. Kong, R. Zhao, X. Wang, *Nanomaterials*, **2025**, *15*, 940.
- [33] Z. Xing, W. Zhao, B. Yu, Y. Wang, L. Zhou, P. Xiong, M. Chen, J. Zhu, *Small*, **2024**, *20*, 2405442.
- [34] Y. Shen, B. Liu, X. Liu, J. Liu, J. Ding, C. Zhong, W. Hu, *Energy Storage Mater.*, **2021**, *34*, 461-474.
- [35] H. Luo, X. Su, Z. Chen, H. Guo, R. Zhao, Q. Gao, M. Lu, T. Liu, *Adv Mater.*, **2025**, DOI:10.1002/adma.202507978.
- [36] T. Liu, X. Dong, J. Zhang, H. Chen, R. Cao, Z. Sun, W. Zhou, H. Li, D. Chao, Z. Zhou, R. Zhao, *Chem. Sci.*, **2025**, *16*, 17426-17435.
- [37] H. Luo, F. Li, M. Wang, S. Sun, M. Zhou, W. Zhang, H. Guo, X. Su, X. Li, L. Ma, *Chem. Sci.*, **2025**, *16*, 2044-2045.
- [38] H. Luo, H. Guo, X. Li, S. Li, Y. Li, J. Shi, Q. Gao, H. He, M. Lu, Q. Zhang, D. Chao, *Matter*, **2025**, DOI:10.1016/j.matt.2025.102379.
- [39] M. Qin, Z. Zeng, S. Cheng, J. Xie, *Interdiscip. Mater.*, **2023**, *2*, 308-336.
- [40] M. Han, T. C. Li, X. Chen, H. Y. Yang, *Small*, **2023**, *20*, 2304901.
- [41] Y. Gao, Z. Wang, H. Tu, J. Xue, S. Weng, S. Lu, L. Liu, G. Sun, K. Peng, X. Zhang, D. Li, Y. Liu, J. Xu, H. Li, X. Wu, *Adv. Funct. Mater.*, **2024**, *35*, 2414652.
- [42] L. Jiang, S. Han, Y.-C. Hu, Y. Yang, Y. Lu, Y.-C. Lu, J. Zhao, L. Chen, Y.-S. Hu, *Nat. Energy*, **2024**, *9*, 839-848.
- [43] G. Yang, X. Xu, G. Qu, J. Deng, Y. Zhu, C. Fang, O. Fontaine, P. Hiralal, J. Zheng, H. Zhou, *Chem. Eng. J.*, **2023**, *455*, 140806.
- [44] X. Ye, X. Xiao, Z. Wu, Y. Zhan, X. Wu, S. Liu, *J. Mater. Chem. A*, **2024**, *12*, 23337-23363.
- [45] Q. Zheng, L. Liu, Z. Hu, Z. Tang, H. Lu, Y. Gao, J. Wang, Y. Song, C. Han, W. Li, *Adv. Funct. Mater.*, **2025**, DOI:10.1002/adfm.202504782.
- [46] C. Zhu, D. Wu, C. Wang, J. Ma, *Adv. Funct. Mater.*, **2024**, *34*, 2406764.
- [47] X. Zheng, Z. Cao, Z. Gu, L. Huang, Z. Sun, T. Zhao, S. Yu, X.-L. Wu, W. Luo, Y. Huang, *ACS Energy Lett.*, **2022**, *7*, 2032-2042.
- [48] Y. Sui, M. Yu, Y. Xu, X. Ji, *J. Electrochem. Soc.*, **2022**, *169*, 030537.
- [49] Y. Wang, H. Wei, Z. Li, X. Zhang, Z. Wei, K. Sun, H. Li, *Chem. Rec.*, **2022**, *22*, e202200132.
- [50] X. Yang, P. Li, C. Guo, W. Yang, N. Zhou, X. Huang, Y. Yang, *J. Power Sources*, **2024**, *624*, 235563.
- [51] F. Yue, Z. Tie, S. Deng, S. Wang, M. Yang, Z. Niu, *Angew. Chem. Int. Ed.*, **2021**, *60*, 13882-13886.
- [52] M. Li, R. Li, H. Ma, M. Yang, Y. Dai, H. Yu, Y. Hao, Z. Wang, B. Wang, M. Hu, J. Yang, *Nano-Micro Lett.*, **2025**, *17*, 158
- [53] J. Wang, Y. Yang, Y. Wang, S. Dong, L. Cheng, Y. Li, Z. Wang, L. Trabzon, H. Wang, *ACS Nano* **2022**, *16*, 15770-15778.
- [54] T. Xiong, Y. Guo, X. Wang, *Adv. Funct. Mater.*, **2024**, *35*, 2421240.
- [55] R. Zhao, X. Dong, P. Liang, H. Li, T. Zhang, W. Zhou, B. Wang, Z. Yang, X. Wang, L. Wang,



- Z. Sun, F. Bu, Z. Zhao, W. Li, D. Zhao, D. Chao, *Adv Mater.*, **2023**, *35*, 2209288. View Article Online
DOI: 10.1039/D5SC08605A
- [56] C. Yang, J. Xia, C. Cui, T. P. Pollard, J. Vatamanu, A. Faraone, J. A. Dura, M. Tyagi, A. Kattan, E. Thimsen, J. Xu, W. Song, E. Hu, X. Ji, S. Hou, X. Zhang, M. S. Ding, S. Hwang, D. Su, Y. Ren, X.-Q. Yang, H. Wang, O. Borodin, C. Wang, *Nat. Sustain.*, **2023**, *6*, 325-335.
- [57] M. Qiu, P. Sun, K. Han, Z. Pang, J. Du, J. Li, J. Chen, Z. L. Wang, W. Mai, *Nat. Commun.*, **2023**, *14*, 601
- [58] L. Jiang, D. Dong, Y.-C. Lu, *Nano Energy*, **2022**, *1*, e9120003.
- [59] T. Xue, Y. Mu, Z. Zhang, J. Guan, J. Qiu, C. Yang, L. Zang, L. Zeng, *Adv. Energy Mater.*, **2025**, *15*, 2500674.
- [60] Y. Liu, J. Chen, M. Qiu, P. Sun, W. Mai, *Adv. Funct. Mater.*, **2025**, DOI:10.1002/adfm.202504127.
- [61] T. Xue, J. Guan, Y. Mu, M. Han, C. Yang, L. Zang, L. Zeng, *Chem. Eng. J.*, **2025**, *514*, 162994.
- [62] Q. Nian, T. Sun, Y. Li, S. Jin, S. Liu, X. Luo, Z. Wang, B. Q. Xiong, Z. Cui, D. Ruan, H. Ji, Z. Tao, X. Ren, *Angew. Chem. Int. Ed.*, **2023**, *62*, e202217671.
- [63] M. Qiu, P. Sun, Y. Liang, J. Chen, Z. L. Wang, W. Mai, *Nat. Commun.*, **2024**, *15*, 10420
- [64] C. Yang, X. Liu, Y. Lin, L. Yin, J. Lu, Y. You, *Adv Mater.*, **2023**, *35*, 2301817.
- [65] M. Wang, M. Zheng, J. Lu, Y. You, *Joule*, **2024**, *8*, 2467-2482.
- [66] S. Deng, B. Xu, J. Zhao, H. Fu, *Energy Storage Mater.*, **2024**, *70*, 103490.
- [67] Q. Dong, H. Ao, Z. Qin, Z. Xu, J. Ye, Y. Qian, Z. Hou, *Small*, **2022**, *18*, 2203347.
- [68] K. Chen, J. Luo, Y. Huang, *Chem. Eng. J.*, **2025**, *503*, 158260.
- [69] L. Geng, J. Meng, X. Wang, W. Wu, K. Han, M. Huang, C. Han, L. Wu, J. Li, L. Zhou, L. Mai, *Chem*, **2025**, *11*, 102302.
- [70] T. Ma, Y. Ni, Q. Wang, W. Zhang, S. Jin, S. Zheng, X. Yang, Y. Hou, Z. Tao, J. Chen, *Angew. Chem. Int. Ed.*, **2022**, *61*, e202207927.
- [71] Z. Wang, T. Zheng, S. Wang, X.-G. Zhang, Y. Gu, S. Tang, Y. Fu, *J. Am. Chem. Soc.*, **2025**, *147*, 5962-5970.
- [72] J. Guo, S. Gu, W. Nie, B. Long, S. Ryazantsev, S. Malyshev, J. Li, S. Guo, C. Wu, *Adv Mater.*, **2025**, *37*, 2419865.
- [73] A. Cushing, T. Zheng, K. Higa, G. Liu, *Polymers*, **2021**, *13*, 4033.
- [74] L. Luo, K. Chen, H. Chen, H. Li, R. Cao, X. Feng, W. Chen, Y. Fang, Y. Cao, *Adv Mater.*, **2023**, *36*, 2308881.
- [75] Q. Nian, T. Sun, S. Liu, H. Du, X. Ren, Z. Tao, *Chem. Eng. J.*, **2021**, *423*, 130253.
- [76] M. Zhao, T. Cheng, T. Li, S. Wang, Y. Yin, X. Li, *Energy Environ. Sci.*, **2025**, *18*, 378-385.
- [77] H.-I. Kim, K. M. Lee, W.-Y. Kim, S. H. Kweon, X. Wang, S. Zheng, S.-H. Kim, J. H. Ha, S. J. Kang, Z.-S. Wu, S. K. Kwak, S.-Y. Lee, *Energy Environ. Sci.*, **2024**, *17*, 1961-1974.
- [78] J. Wei, P. Zhang, J. Sun, Y. Liu, F. Li, H. Xu, R. Ye, Z. Tie, L. Sun, Z. Jin, *Chem. Soc. Rev.*, **2024**, *53*, 10335-10369.
- [79] Y. Feng, L. Zhou, H. Ma, Z. Wu, Q. Zhao, H. Li, K. Zhang, J. Chen, *Energy Environ. Sci.*, **2022**, *15*, 1711-1759.
- [80] D. Sui, R. Luo, S. Xie, H. Zhang, T. Ma, H. Sun, T.-T. Jia, J. Sun, X. Li, *Chem. Eng. J.*, **2024**, *480*, 148007.
- [81] D. Guo, S. Thomas, J. K. El-Demellawi, Z. Shi, Z. Zhao, C. G. Canlas, Y. Lei, J. Yin, Y. Zhang, M. N. Hedhili, M. Arsalan, Y. Zhu, O. M. Bakr, O. F. Mohammed, H. N. Alshareef, *Energy Environ. Sci.*, **2024**, *17*, 8151-8161.



- [82] Y. Shang, N. Chen, Y. Li, S. Chen, J. Lai, Y. Huang, W. Qu, F. Wu, R. Chen, *Adv Mater.*, **2020**, 32, 2004017. View Article Online
DOI: 10.1039/D5SC08605A
- [83] Z. Chen, Y. Wang, Q. Wu, C. Wang, Q. He, T. Hu, X. Han, J. Chen, Y. Zhang, J. Chen, L. Yang, X. Wang, Y. Ma, J. Zhao, *Adv Mater.*, **2024**, 36, 2411004.
- [84] H. Zhang, Y. Zhong, J. Li, Y. Liao, J. Zeng, Y. Shen, L. Yuan, Z. Li, Y. Huang, *Adv. Energy Mater.*, **2022**, 13, 2203254.
- [85] Z. Hao, X. Shi, Z. Yang, L. Li, S. L. Chou, *Adv. Funct. Mater.*, **2022**, 32, 2208093.
- [86] M. Luo, H. Yu, F. Hu, T. Liu, X. Cheng, R. Zheng, Y. Bai, M. Shui, J. Shu, *Chem. Eng. J.*, **2020**, 380, 122557.
- [87] X. Yun, Y. Chen, H. Gao, D. Lu, L. Zuo, P. Gao, G. Zhou, C. Zheng, P. Xiao, *Adv. Energy Mater.*, **2024**, 14, 2304341.
- [88] M. Wang, L. Yin, M. Zheng, X. Liu, C. Yang, W. Hu, J. Xie, R. Sun, J. Han, Y. You, J. Lu, *Nat. Commun.*, **2024**, 15, 8866
- [89] X. Luo, R. Wang, L. Zhang, Z. Liu, H. Li, J. Mao, S. Zhang, J. Hao, T. Zhou, C. Zhang, *ACS Nano*, **2024**, 18, 12981-12993.
- [90] Y. Zhang, S. Shen, K. Xi, P. Li, Z. Kang, J. Zhao, D. Yin, Y. Su, H. Zhao, G. He, S. Ding, *Angew. Chem. Int. Ed.*, **2024**, 63, e202407067.
- [91] Y. Fu, X. Cui, Y. Zhang, T. Feng, J. He, X. Zhang, X. Bai, Q. Cheng, *Chem. Eng. Data*, **2018**, 63, 1180-1189.
- [92] B. S. Lalia, N. Yoshimoto, M. Egashira, M. Morita, *J. Power Sources*, **2010**, 195, 7426-7431.
- [93] B. Batiot, T. Rogaume, F. Richard, J. Luche, A. Collin, E. Guillaume, J. L. Torero, *Appl. Sci.*, **2021**, 11, 4075.
- [94] L. Sun, Z. Song, C. Deng, Q. Wang, F. Mo, H. Hu, G. Liang, *Batteries*, **2023**, 9, 386.
- [95] J. Landesfeind, H. A. Gasteiger, *J. Electrochem. Soc.*, **2019**, 166, A3079-A3097.
- [96] G. Kucinskis, M. Bozorgchenani, M. Feinauer, M. Kasper, M. Wohlfahrt-Mehrens, T. Waldmann, *J. Power Sources*, **2022**, 549, 232129.
- [97] M. Chen, G. Chen, C. Sun, X. Li, M. Zhang, H. Hua, J. Zhao, Y. Yang, *Angew. Chem. Int. Ed.*, **2025**, 64, e202502005.
- [98] W. Mei, Z. Liu, C. Wang, C. Wu, Y. Liu, P. Liu, X. Xia, X. Xue, X. Han, J. Sun, G. Xiao, H.-y. Tam, J. Albert, Q. Wang, T. Guo, *Nat. Commun.*, **2023**, 14, 5251
- [99] J. Hou, L. Lu, L. Wang, A. Ohma, D. Ren, X. Feng, Y. Li, Y. Li, I. Ootani, X. Han, W. Ren, X. He, Y. Nitta, M. Ouyang, *Nat. Commun.*, **2020**, 11, 5100
- [100] M. Yang, Z. Yan, J. Xiao, W. Xin, L. Zhang, H. Peng, Y. Geng, J. Li, Y. Wang, L. Liu, Z. Zhu, *Angew. Chem. Int. Ed.*, **2022**, 61, e202212666.
- [101] C. Xie, S. Liu, H. Wu, Q. Zhang, C. Hu, Z. Yang, H. Li, Y. Tang, H. Wang, *Sci. Bull.*, **2023**, 68, 1531-1539.
- [102] A. Naveed, H. Yang, J. Yang, Y. Nuli, J. Wang, *Angew. Chem. Int. Ed.*, **2019**, 58, 2760-2764.
- [103] B. Hu, T. Chen, Y. Wang, X. Qian, Q. Zhang, J. Fu, *Adv. Energy Mater.*, **2024**, 14, 2401470.
- [104] Q. Guo, R. Luo, Z. Tang, X. Li, X. Feng, Z. Ding, B. Gao, X. Zhang, K. Huo, Y. Zheng, *ACS Nano*, **2023**, 17, 24227-24241.
- [105] Y. Quan, M. Yang, M. Chen, W. Zhou, X. Han, J. Chen, B. Liu, S. Shi, P. Zhang, *Chem. Eng. J.*, **2023**, 458, 141392.
- [106] C. Liu, X. Xie, B. Lu, J. Zhou, S. Liang, *ACS Energy Lett.*, **2021**, 6, 1015-1033.
- [107] D. Feng, F. Cao, L. Hou, T. Li, Y. Jiao, P. Wu, *Small*, **2021**, 17, 2103195.



- [108] Y. An, C. Shu, Y. Liu, Y. Xu, L. Kang, X. Zhang, J. Sun, Z. Ma, K. Zhao, Y. Huang, F. Kang, F. Jiang, W. Liu, *ACS Nano*, **2025**, *19*, 11146-11163. View Article Online
DOI: 10.1039/D5SC08605A
- [109] S. Lin, H. Hua, P. Lai, J. Zhao, *Adv. Energy Mater.*, **2021**, *11*, 2101775.
- [110] Y. Jiang, B. Wujieti, Y. Liu, Q. Zeng, Z. Li, J. Guan, H. Wang, L. Chen, Y. Cao, R. Li, Y. Zhou, H. Zhou, W. Cui, L. Zhang, *Adv. Funct. Mater.*, **2024**, *35*, 2421160.
- [111] W. Chen, Y. Wang, F. Wang, Z. Zhang, W. Li, G. Fang, F. Wang, *Adv Mater.*, **2024**, *36*, 2411802.
- [112] S. Huang, Z. Li, P. Li, X. Du, M. Ma, Z. Liang, Y. Su, L. Xiong, *J. Mater. Chem. A*, **2023**, *11*, 15532-15539.
- [113] S. Wang, Z. Xue, F. Chu, Z. Guan, J. Lei, F. Wu, *J. Energy Chem.*, **2023**, *79*, 201-210.
- [114] X. Wang, Z. Xi, Q. Zhao, *Ind. Chem. Mater.*, **2025**, *3*, 7-30.
- [115] L. Geng, J. Meng, X. Wang, C. Han, K. Han, Z. Xiao, M. Huang, P. Xu, L. Zhang, L. Zhou, L. Mai, *Angew. Chem. Int. Ed.*, **2022**, *61*, e202206717.
- [116] X. Zhang, R. Wang, Z. Liu, Q. Ma, H. Li, Y. Liu, J. Hao, S. Zhang, J. Mao, C. Zhang, *Adv. Energy Mater.*, **2024**, *14*, 2400314.
- [117] X. Zhou, Q. Zhang, Z. Zhu, Y. Cai, H. Li, F. Li, *Angew. Chem. Int. Ed.*, **2022**, *61*, e202205045.
- [118] Y. Jie, S. Wang, S. Weng, Y. Liu, M. Yang, C. Tang, X. Li, Z. Zhang, Y. Zhang, Y. Chen, F. Huang, Y. Xu, W. Li, Y. Guo, Z. He, X. Ren, Y. Lu, K. Yang, S. Cao, H. Lin, R. Cao, P. Yan, T. Cheng, X. Wang, S. Jiao, D. Xu, *Nat. Energy*, **2024**, *9*, 987-998.
- [119] M. Liu, W. Yuan, G. Ma, K. Qiu, X. Nie, Y. Liu, S. Shen, N. Zhang, *Angew. Chem. Int. Ed.*, **2023**, *62*, e202304444.
- [120] Z. Chen, B. Wang, Y. Li, F. Bai, Y. Zhou, C. Li, T. Li, *ACS Appl. Mater. Interfaces*, **2022**, *14*, 28014-28020.
- [121] D.-Y. Wang, E. Hu, G. Wu, H. Choo, C. Franke, B.-E. Jia, J. Song, A. Sumboja, I. T. Anggraningrum, A. Z. Syahril, Q. Zhu, M.-F. Ng, T. Li, Q. Yan, *Angew. Chem. Int. Ed.*, **2025**, *64*, e202508641.
- [122] X. Shi, J. Xie, J. Wang, S. Xie, Z. Yang, X. Lu, *Nat. Commun.*, **2024**, *15*, 302
- [123] Q. Wang, C. Zhao, J. Wang, Z. Yao, S. Wang, S. G. H. Kumar, S. Ganapathy, S. Eustace, X. Bai, B. Li, M. Wagemaker, *Nat. Commun.*, **2023**, *14*, 440
- [124] H. Ji, C. Xie, T. Wu, H. Wang, Z. Cai, Q. Zhang, W. Li, L. Fu, H. Li, H. Wang, *Chem. Commun.*, **2023**, *59*, 8715-8718.
- [125] Z. J. Chen, T. Y. Shen, X. Xiao, X. C. He, Y. L. Luo, Z. Jin, C. H. Li, *Adv Mater.*, **2024**, *36*, 2413268.
- [126] Y. Liu, F. Li, J. Hao, H. Li, S. Zhang, J. Mao, T. Zhou, R. Wang, L. Zhang, C. Zhang, *Adv. Funct. Mater.*, **2024**, *34*, 2400517.



Data availability

All data needed to evaluate the conclusions in the paper are present in the paper.

